Performance Analysis of an Island Power System Including Wind Turbines Operating under Random Wind Speed

Meng-Jen Chen, Yu-Chi Wu, Guo-Tsai Liu, and Sen-Feng Lin

Abstract—With continuous rise of oil price, how to develop alternative energy source has become a hot topic around the world. This study discussed the dynamic characteristics of an island power system operating under random wind speed lower than nominal wind speeds of wind turbines. The system primarily consists of three diesel engine power generation systems, three constant-speed variable-pitch wind turbines, a small hydraulic induction generation system, and lumped static loads. Detailed models based on Matlab/Simulink were developed to cater for the dynamic behavior of the system. The results suggested this island power system can operate stably in this operational mode. This study can serve as an important reference for planning, operation, and further expansion of island power systems.

Keywords—Diesel engine power generation system, constant-speed variable-pitch wind turbine, small hydraulic induction generation system, penetration, Matlab/Simulink, SimPowerSystems.

I. INTRODUCTION

IN recent years, with continuous rise of oil price, how to develop alternative energy source has become a hot topic around the world. After the Kyoto Protocol has been exercised, a new trend of international environment protection has emerged, and various industries in Taiwan have proposed suggestions for new energy policy. Since "The 2nd National Energy Conference," the government has set CO_2 control mechanism actively and expected decrease of 38 million MT by the end of 2015, 58.68 million MT by 2020, and 78.41 million MT by 2025. The utilization of renewable energy is expected to reach 7,000~8,000MW by 2020 and 8,000~9,000MW by 2025, to attain the goal for total installed capacity penetration 12% or energy structure penetration 4~6%. The renewable energy development projects include biomass, wind power, photovoltaic system, solar heat, hydrogen energy, fuel cell, oceanic energy, geothermal heat, etc. The projects also cover planning offshore wind farms with scale of economy and fostering the development of the domestic wind industry [1].

Diesel engine power generation systems are commonly used to supply relatively small capacity systems such as island power systems, industrial power systems, and marine power systems. Especially, in many remote regions or islands, the electric power from central power stations is difficult to be transmitted to these places. The diesel engine power generation becomes the most commonly used power generation technology in these regions because the diesel engine has advantages of easy start-up, low equipment cost, short plant construction period, and stable voltage and frequency control. However, the power quality problem resulted from small capacity ratio between the power generation system and load has to be concerned. Combining the diesel engine with other renewable energy power supplies to form a hybrid system to maintain acceptable power quality and reliable electricity supply is an economical way to reduce the fuel cost and the pollution caused by fossil fuels [2], [3].

Many studies have been done on island power systems and hybrid power systems. Reference [4] proposed an algorithm for optimizing the assemblies of stand-alone wind-diesel hybrid power generation system and used a prototype system to verify the dynamic characteristics of two generators under optimal load distribution. Reference [5] discussed the power quality problem of a stand-alone island power system with high penetration of wind energy and indicated that the torque variation in diesel engine was the main cause for voltage flicker. Reference [6] proposed an automatic reactive power control strategy for stand-alone wind-diesel hybrid power system which consisted of a wind power generation system with permanent magnet generator and a diesel engine power generation system with synchronous generator. Reference [7] discussed the dynamic behavior simulation of a hybrid system comprising diesel engine and variable-speed wind turbine and proved that the power quality could be improved by controlling the frequency. Reference [8] discussed the dynamic characteristics of wind-diesel hybrid systems used in remote regions, including coupling problem, mutual interference of interconnected systems, improvement on reactive power, reduction of wind turbine output loss, etc. Reference [9] analyzed and designed the control method for a stand-alone wind-diesel hybrid system at different frequencies. Reference [10] discussed the influence of power quality on the wind-diesel hybrid system and the problems caused by load and frequency switching. Reference [11] used genetic algorithm to adjust static reactive power compensator, so the system could control the reactive power within an ideal range automatically. Reference [12] discussed the control system used for wind-diesel hybrid system with high wind power. Few of these

Meng-Jen Chen is with the Department of Electrical Engineering, National Kaohsiung University of Applied Sciences, Kaohsiung, Taiwan (e-mail: mengjen@cc.kuas.edu.tw).

Yui-Chi Wu is with the Department of Electrical Engineering, National United University, Miao-Li, Taiwan (corresponding author: +886-37-381362; fax: +886-37-327887; e-mail: ycwu@nuu.edu.tw).

Guo-Tsai Liu and Sen-Feng Lin are with the Department of Electrical Engineering, National Kaohsiung University of Applied Sciences, Kaohsiung, Taiwan.

studies have used detailed dynamic pitch-control models to analyze the dynamic characteristics of an island power system with high renewable energy penetration.

This study discussed the dynamic characteristics of an island power system under random wind speed. This study is essential for planning, operation, and further expansion of island power systems.

II. ISLAND POWER SYSTEM

A. Configuration of an Island Power System

Fig. 1 shows the configuration of a simplified island power system. The system consists of three diesel engine power generation systems, three constant-speed variable-pitch wind turbines, a small hydraulic inductive generation system, and lumped static loads. Each diesel engine power generation system is rated 5MVA, consisting of a diesel engine, a synchronous generator, an excitation system, and a transformer. Each constant-speed variable-pitch wind turbine is rated 2MW, consisting of blades, a mechanical transmission system, an induction generator, and a transformer. The small hydraulic power generation system is rated 1MVA, consisting of a small hydraulic turbine, an induction generator, and a transformer. The diesel engine power generation systems are the main power sources, and the output voltage is 11.4kV. The minimum load of this system is 4MVA, and the maximum load is 12MVA.
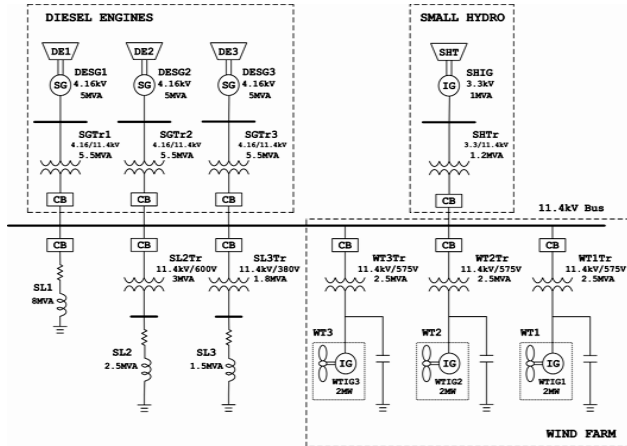

Fig. 1 Configuration of a simplified island power system

B. Diesel Engine Model

The diesel engine prime mover model is usually developed by using the engine performance data provided by the manufacturer. Fig. 2 shows the schematic diagram of a diesel engine prime mover. This model consists of three subsystems-- thermodynamic model, speed governing model, and shaft model [13].
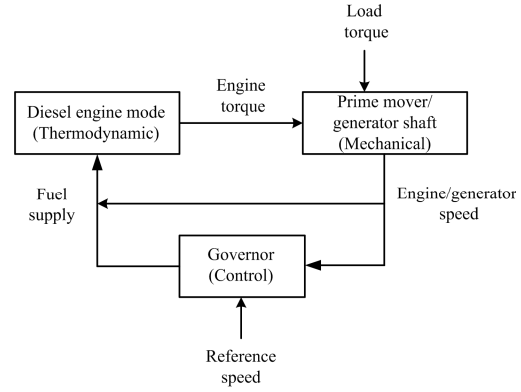

Fig. 2 Schematic diagram of a diesel engine prime mover

Under normal circumstances, the engine torque is proportional to the fuel. In the case of sufficient air supply, the fuel can be combusted completely, so the torque can be regarded as proportional to the fuel tank level. However, in the case of transient and heavy load, the fuel cannot be combusted completely, and the torque is limited to the air supply. The turbocharger is usually installed to improve the situation.

The speed adjustment is implemented by the speed governing system of prime mover. When the generator speed deviates from the rated speed, the governor mechanism will detect the variation in rotational speed. The position of transfer valve is changed and the output of prime mover is adjusted to make the speed steady. Fig. 3 shows the block diagram of typical governing arrangement.
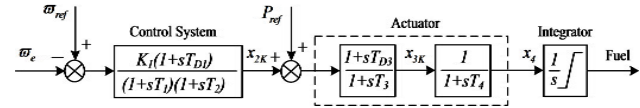

Fig. 3 Block diagram of typical governing arrangement

The state equation of this diagram can be expressed as

$$p \begin{bmatrix} x_1 \\ x_2 \\ x_3 \\ x_4 \end{bmatrix} = \begin{bmatrix} \frac{-1}{T_1} & 0 & 0 & 0 \\ \frac{1}{T_2} & \frac{-1}{T_2} & 0 & 0 \\ \frac{KT_{D1}}{T_2 T_3} & \frac{K(T_2 - T_{D1})}{T_2 T_3} & \frac{-1}{T_3} & 0 \\ \frac{KT_{D1}T_{D3}}{T_2 T_3 T_4} & \frac{KT_{D3}(T_2 - T_{D1})}{T_2 T_3 T_4} & \frac{T_3 - T_{D3}}{T_3 T_4} & \frac{-1}{T_4} \end{bmatrix} \begin{bmatrix} x_1 \\ x_2 \\ x_3 \\ x_4 \end{bmatrix} + \begin{bmatrix} \frac{-1}{T_1} & \frac{1}{T_1} & 0 & 0 \\ 0 & 0 & 0 & 0 \\ 0 & 0 & \frac{1}{T_3} & 0 \\ 0 & 0 & \frac{KT_{D3}}{T_3 T_4} & 0 \end{bmatrix} \begin{bmatrix} \varpi_e \\ \varpi_{ref} \\ P_{ref} \\ 0 \end{bmatrix} \tag{1}$$

$$x_{2K} = K[\frac{T_{D1}}{T_2}x_1 + (1 - \frac{T_{D1}}{T_2})x_2] \tag{2}$$

$$x_{3K} = \frac{KT_{D1}T_{D3}}{T_2 T_3}x_1 + \frac{KT_{D3}(1 - T_{D1})}{T_2 T_3}x_2 + \frac{T_3 - T_{D3}}{T_3}x_3 + \frac{T_{D3}}{T_3}P_{ref} \tag{3}$$

where ω_e is the engine speed, ω_{ref} is the reference rotational speed, P_{ref} is the reference power.

The mechanical shaft model can be represented by the torsional model of a simple two-mass system as shown in Fig. 4 [14]. As the system is represented by second-order differential

equations in angular displacement θ_1 of mass 1 and angular displacement θ_2 of mass 2, the system will have the undamped natural frequency given by $(\pi/2)(D/J_1+D/J_2)^{1/2}$.

This system can be expressed as

$$p\begin{bmatrix} \theta_1 \\ \omega_1 \\ \theta_2 \\ \omega_2 \end{bmatrix} = \begin{bmatrix} 0 & 1 & 0 & 0 \\ \dfrac{-D}{J_1} & \dfrac{-C_1-C_{12}}{J_1} & \dfrac{D}{J_1} & \dfrac{C_{12}}{J_1} \\ 0 & 0 & 0 & 1 \\ \dfrac{D}{J_2} & \dfrac{C_{12}}{J_2} & \dfrac{-D}{J_2} & \dfrac{-C_2-C_{12}}{J_2} \end{bmatrix} \begin{bmatrix} \theta_1 \\ \omega_1 \\ \theta_2 \\ \omega_2 \end{bmatrix} + \begin{bmatrix} 0 & 0 & 0 & 0 \\ \dfrac{1}{J_1} & \dfrac{-1}{J_1} & 0 & 0 \\ 0 & 0 & 0 & 0 \\ 0 & 0 & \dfrac{-1}{J_2} & \dfrac{-1}{J_2} \end{bmatrix} \begin{bmatrix} \tau_1 \\ \tau_{b1} \\ \tau_2 \\ \tau_{b2} \end{bmatrix} \quad (4)$$

where J_1 is the inertia of rotating mass 1 including coupling, J_2 is the inertia of rotating mass 1 including coupling, D_1 is the stiffness of shaft 1, D_2 is the stiffness of shaft 2, C_1 is the damping coefficient of mass 1, C_2 is the damping coefficient of mass 2, C_{12} is the mutual damping coefficient of mass 1 and mass 2, τ_{b1} is the bearing loss torque of mass 1, τ_{b2} is the bearing loss torque of mass 2, and D is the sum of D_1 and D_2.
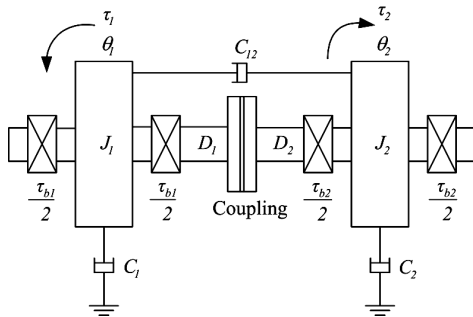

Fig. 4 Torsional model of a two-mass system

C. Constant-Speed Variable-Pitch Wind Turbine Model

The air flow produces wind pressure to rotate wind turbine blades, and the mechanical power is delivered to the generator through the transmission system. Therefore, the order of wind energy conversion is that the kinetic energy of wind is converted into mechanical energy and then into electric energy. The principle for blade pitch angle control includes comparing the real power of wind turbine with the reference power, sending the signal to a gain, limiting the upper and lower limits of the value, and adjusting the wind turbine blade pitch angle. The reference power can be determined by the wind turbine power curve.

According to the aerodynamics, the wind turbine output power can be expressed as

$$P_w = c_p(\lambda,\beta)\frac{\rho A}{2}v_{wind}^3 \quad (5)$$

$$c_p = c_1(c_2 - c_3\beta - c_4\beta^{1.5} - c_5)e^{-c_6(\lambda,\beta)} \quad (6)$$

where λ is the blade tip speed ratio, β is the blade pitch angle, ρ is the air density, A is the blade swept area, v_{wind} is the wind velocity, and c_p is the power coefficient, c_1=0.5, c_2=116/λ_i,

c_3=0.4, c_4=0, c_5=5, c_6=21/λ_i, $\dfrac{1}{\lambda_i} = \dfrac{1}{\lambda + 0.08\beta} - \dfrac{0.035}{\beta^3 + 1}$ [15].

The random wind speed employed in this study can be expressed as

$$V_{WN} = 2\sum_{i=1}^{N}[S_V(\omega_i)\Delta\omega]^{1/2}\cos(\omega_i t + \phi_i) \quad (7)$$

$$\omega_i = (i-1/2)\Delta\omega \quad (8)$$

$$S_V(\omega_i) = \frac{2K_N F^2|\omega_i|}{\pi^2[1+(F\omega_i/\mu\pi)^2]^{4/3}} \quad (9)$$

where ϕ_i is a random distribution value between 0 and 2π, K_N is surface resistance coefficient, F is scale of disturbance, μ is the average wind speed in m/s [16]. Reference [16] suggested that there will be relatively good results for disturbance wind simulation in the case of N equal to 50 and $\Delta\omega$ between 0.5 and 2.0rad/s.

D. Small Hydraulic Turbine Model

Small hydro power is an environmental friendly energy resource. It is clean, renewable and can be made to be unobtrusive. In addition, hydro turbines are associated with low maintenance and long life and produce energy which reduces the use of fossil fuel. Within the category of small hydro plant a wide range of turbine types are available.

Simpler modeling procedure for small hydro turbines in conjunction with induction generators have been validated in practice over a number of years. Fig. 5 shows the output torque versus speed for a mid-range unit when the input torque is a constant. Apply a curve-fitting technique; the torque-speed curve can be represented by a polynomial for simulation.
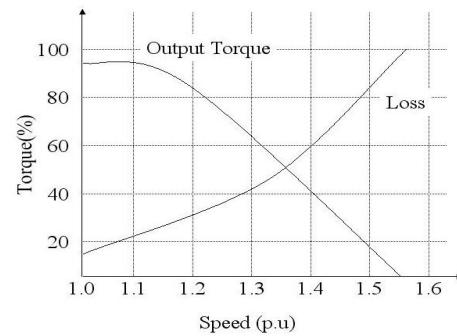

Fig. 5 Characteristics of the small-hydro turbine prime mover

E. Synchronous Generator Model

A synchronous generator requires a prime mover to supply mechanical power and an excitation system to supply excitation voltage when it is in operation. The stator structure of a synchronous generator is three-phase symmetrical, and the rotor structure is either salient or cylindrical. The voltage equation of a synchronous generator referring to rotor can be expressed as

$$\begin{bmatrix} v_{qs} \\ v_{ds} \\ v_{kq} \\ v_{fd} \\ v_{kd} \end{bmatrix} = \begin{bmatrix} -r_s - pL_q & -\omega_r L_d & pL_{mq} & \omega_r L_{md} & \omega_r L_{md} \\ \omega_r L_q & -r_s - pL_d & -\omega_r L_{mq} & pL_{md} & pL_{md} \\ -pL_{mq} & 0 & r_{kq} + pL_{kq} & 0 & 0 \\ 0 & -pL_{md} & 0 & r_{fd} + pL_{fd} & pL_{md} \\ 0 & -pL_{md} & 0 & pL_{md} & r_{kd} + pL_{kd} \end{bmatrix} \begin{bmatrix} i_{qs} \\ i_{ds} \\ i_{kq} \\ i_{fd} \\ i_{kd} \end{bmatrix} \quad (10)$$

where v_{ds} and i_{ds} are the d-axis stator voltage and current, v_{qs} and i_{qs} are the q-axis stator voltage and current, v_{kq} and i_{kq} are the q-axis damper winding voltage and current, v_{fd}, v_{kd}, i_{fd} and i_{kd} are the excitation voltage, d-axis damper winding voltage, exciting current and d-axis damper winding current, r_s, r_{fd}, r_{kd} and r_{kq} are the stator resistance, excitation winding resistance, d-axis damper winding resistance and q-axis damper winding resistance, L_d, L_q, L_{fd}, L_{kd} and L_{kq} are the d-axis inductance, q-axis inductance, excitation winding inductance, d-axis damper winding inductance and q-axis damper winding inductance, L_{md} and L_{mq} are the d-axis mutual inductance and q-axis mutual inductance, and p is the differential operand [17], [18]. In addition, the electromagnetic torque generated by the synchronous generator can be expressed as

$$T_e = \frac{3}{2} n [L_{md} (-i_{ds} + i_{fd} + i_{kd}) i_{qs} - L_{mq} (-i_{qs} + i_{kq}) i_{ds}] \quad (11)$$

where n is the number of pole pairs.

F. Excitation System Model

Almost all synchronous generators operate with automatic voltage regulator (AVR) to control the generator terminal voltage. As soon as a deviation in terminal voltage is detected, the AVR should act to regulate the excitation voltage to control the terminal voltage of the synchronous generator within preset limit. Fig. 6 shows the block diagram of IEEE Type 1 AVR model [19], [20]. The mathematical model for this diagram may be accommodated by the state-space equation as

$$p \begin{bmatrix} x_1 \\ x_2 \\ x_3 \\ x_4 \end{bmatrix} = \begin{bmatrix} \frac{-1}{T_R} & 0 & 0 & 0 \\ \frac{-K_A}{T_A} & \frac{-1}{T_A} & 0 & \frac{-K_A}{T_A} \\ 0 & 0 & \frac{-(K_E + S_E)}{T_E} & 0 \\ 0 & 0 & \frac{-K_F(K_E + S_E)}{T_E T_F} & \frac{-1}{T_F} \end{bmatrix} \begin{bmatrix} x_1 \\ x_2 \\ x_3 \\ x_4 \end{bmatrix} + \begin{bmatrix} \frac{1}{T_R} & 0 & 0 & 0 \\ 0 & \frac{K_A}{T_A} & 0 & 0 \\ 0 & 0 & \frac{1}{T_E} & 0 \\ 0 & 0 & 0 & \frac{K_F}{T_E T_F} \end{bmatrix} \begin{bmatrix} v_T \\ v_{ref} \\ x_{2L} \\ x_{2L} \end{bmatrix} \quad (12)$$
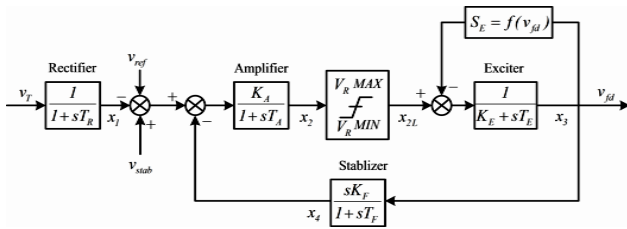

Fig. 6 Block diagram of IEEE Type1 excitation control system

G. Induction Generator Model

A three-phase induction machine has three symmetrical windings on the stator and squirrel-cage shaped conductors or symmetrical windings on the rotor. With all electrical variables

and parameters of the machine referred to the stator, the voltage equation for the induction machine in the two-axis stationary reference frame can be expressed as

$$\begin{bmatrix} v_{qs} \\ v_{ds} \\ v_{qr} \\ v_{dr} \end{bmatrix} = \begin{bmatrix} r_s + pL_{ss} & 0 & pL_m & 0 \\ 0 & r_s + pL_{ss} & 0 & pL_m \\ pL_m & -\omega_r L_m & r_r + pL_{rr} & -\omega_r L_{rr} \\ \omega_r L_m & pL_m & \omega_r L_{rr} & r_r + pL_{rr} \end{bmatrix} \begin{bmatrix} i_{qs} \\ i_{ds} \\ i_{qr} \\ i_{dr} \end{bmatrix} \quad (13)$$

where v_{ds} and i_{ds} are the d-axis stator voltage and current, v_{qs} and i_{qs} are the q-axis stator voltage and current, v_{dr} and i_{dr} are the d-axis rotor voltage and current, v_{qr} and i_{qr} are the q-axis rotor voltage and current, r_s and r_r are the stator resistance and rotor resistance, L_{ss} and L_{rr} are the stator inductance and rotor inductance, L_m is the magnetizing inductance, and p is the differential operand [17], [18]. In addition, the electromagnetic torque of induction generator can be expressed as

$$T_e = \frac{3}{2} n L_m (i_{qs} i_{dr} - i_{ds} i_{qr}) \quad (14)$$

where n is the number of pole pairs.

H. Three-Phase Transformer Model

The transformer transfers energy from one voltage level to another voltage level at the same frequency. The voltage equation of a three-phase transformer can be expressed as

$$\begin{bmatrix} v_{q1} \\ v_{d1} \\ v_{q2} \\ v_{d2} \end{bmatrix} = \begin{bmatrix} r_1 + pL_{11} & 0 & pL_m & 0 \\ 0 & r_1 + pL_{11} & 0 & pL_m \\ pL_m & 0 & r_2 + pL_{22} & 0 \\ 0 & pL_m & 0 & r_2 + pL_{22} \end{bmatrix} \begin{bmatrix} i_{q1} \\ i_{d1} \\ i_{q2} \\ i_{d2} \end{bmatrix} \quad (15)$$

where v_{d1} and i_{d1} are the d-axis primary voltage and current, v_{q1} and i_{q1} are the q-axis primary voltage and current, v_{d2} and i_{d2} are the d-axis secondary voltage and current, v_{q2} and i_{q2} are the q-axis secondary voltage and current, r_1 and r_2 are the primary resistance and secondary resistance, L_{11} and L_{22} are the primary self-inductance and secondary self-inductance, L_m is the magnetizing inductance, and p is the differential operand [17], [18].

I. Static Load Model

The lumped static load can be considered as resistive and inductive load, and the voltage equation can be expressed as

$$\begin{bmatrix} v_{qk} \\ v_{dk} \end{bmatrix} = \begin{bmatrix} r_{sk} + pL_{sk} & 0 \\ 0 & r_{sk} + pL_{sk} \end{bmatrix} \begin{bmatrix} i_{qk} \\ i_{dk} \end{bmatrix} \quad (16)$$

where v_{dk} and i_{dk} are the d-axis voltage and current, v_{qk} and i_{qk} are the q-axis voltage and current, r_{sk} and L_{sk} are the resistance and inductance, and p is the differential operator [17], [18].

III. SIMULATIONS

A. SimPowerSystems Model for the Island Power System

Fig. 7 shows the SimPowerSystems model for the island power system depicted in Fig. 2. It consists of four parts-- part A: diesel engine power generation system module, part B: small hydraulic power generation system module, part C: wind turbine module, and part D: load module [21], [22].

B.Operational Sequence

Three diesel engine power generation sets were connected in parallel at 0 sec, the static load SL1 was connected at 1sec, the static loads SL2 and SL3 were connected at 5sec, the small hydraulic power generation system and the first wind turbine were added at 10sec, the second wind turbine was added at 20 sec, and the third wind turbine was added at 30sec. Total simulation time was 60 seconds.

C.Simulation Results

All the variables are expressed in per unit on the basis of their own capacities. The performance of only one diesel engine power generation system is given because of their identical parameters. The electric power and current are expressed as positive values for the synchronous generator while exporting and as negative values while importing. However, the notation for the induction machine and for the primary side of a transformer is opposite to that for the synchronous machine.

Fig. 8 gives the variations of variables of the first diesel engine power generation system. Fig. 8 (a) indicates the mechanical power of the engine increased when loads were added and decreased when renewable power generation systems were connected. Fig. 8 (b) shows the generator speed dropped when loads were added and then restored to synchronous speed. The figure also shows the generator speed rose temporarily because the renewable energy power generation systems shared part of the active power supplied by the diesel engine generator and restored to synchronous speed due to the adjustment of governing system. Fig. 8 (c) shows the output active power of the generator varied coincidently with the input mechanical power delivered by the diesel engine. Fig. 8 (d) shows the output reactive power of the diesel engine generator increased when static loads were imported within 10 seconds. The figure also shows the reactive power of the generator did not increase significantly when renewable energy power generation systems were connected. Fig. 8 (e) shows the terminal voltage of the diesel generator had obvious transient when the static loads and other power generation systems were connected, but it became stable at 1.0pu soon. Fig. 8 (f) shows the diesel generator excitation voltage varies with the fluctuation of the terminal voltage. The excitation voltage rises, when the terminal voltage drops; the excitation voltage drops, when the terminal voltage rises.
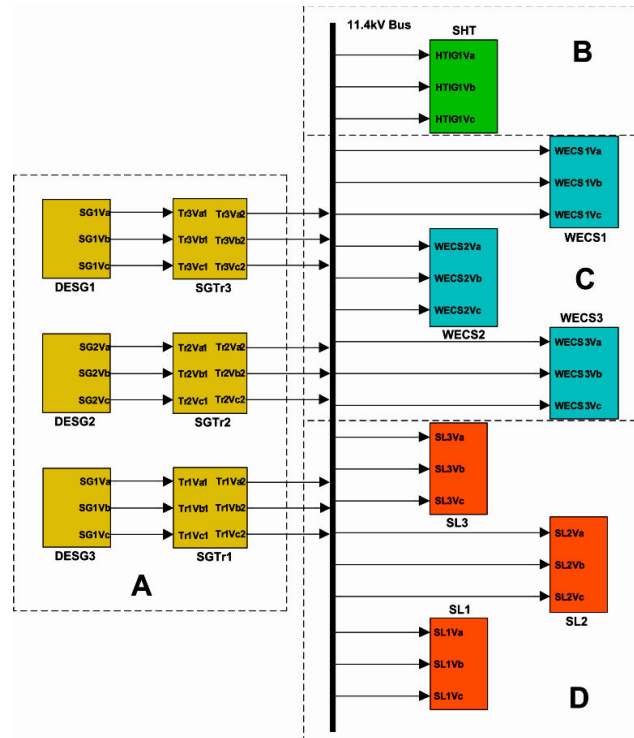

Fig. 7 Configuration of the SimPowerSystems model for the island power system

Fig. 9 gives the variations of variables of the small hydraulic power generation system. Fig. 9 (a) shows the output power of the turbine increased to 0.9pu after 10 sec. Fig. 9 (b) shows the output active power of small hydraulic induction generator varied with the input mechanical power of prime mover, and there was obvious transient when the wind turbines were connected. Fig. 9 (c) shows the output reactive power of the induction generator approached to 0 after transient due to the contribution from power factor compensation device. Fig. 9 (d) shows the terminal voltage of induction generator had obvious transient caused by the connection of wind turbines. Fig. 9 (e) shows the electromagnetic torque of induction generator was negative and varied with the voltage and the mechanical torque of prime mover. Fig. 9 (f) shows the induction generator speed was higher than synchronous speed by about 2.7%.

Fig. 10 gives the variations of variables in the transformer and static loads. Figs. 10 (a) and (b) indicate the changes of active power and reactive power of step-up transformer had the same pattern as those of the generator respectively. Fig. 10 (c) shows the active power of static load SL1 was affected by the terminal voltage, and the reactive power was little as shown in Fig. 10 (d). Figs. 10 (e) and (f) show the changes in active power and reactive power of static load SL2 were similar to SL1.

Fig. 11 gives the variations of variables of the first wind turbine. Fig. 11 (a) shows the wind speed varies within 8-12m/s for a sampling time 2 seconds, apparently less than the nominal wind speed 15m/s. Fig. 11 (b) shows the active power varied with the wind speed, and the reactive power approached to 0

due to the contribution from power factor compensation device as shown in Fig. 11 (c). Fig. 11 (d) shows the pitch angle maintained because the output power was less than the nominal value. Fig. 11 (e) shows the torque of induction machine varied to balance the mechanical torque from wind turbine. Fig. 11 (f) shows the speed of induction machine was higher than synchronous speed.
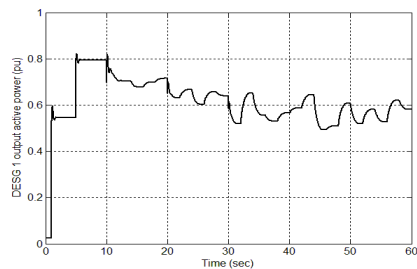
Figs. 12 and 13 give the variations of variables of the second and the third wind turbines. The characteristics of the turbines were similar to those of the first wind turbine with different wind speed and switching time.
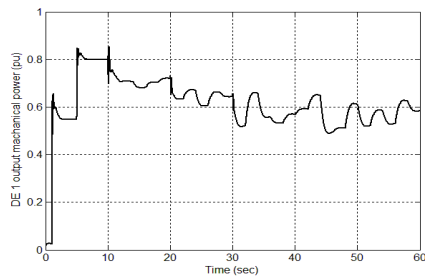
(a) DE1 mechanical power
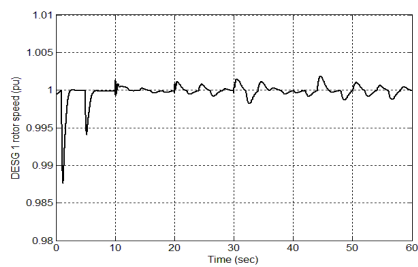
(b) DESG1 rotor speed

(c) DESG1 active power
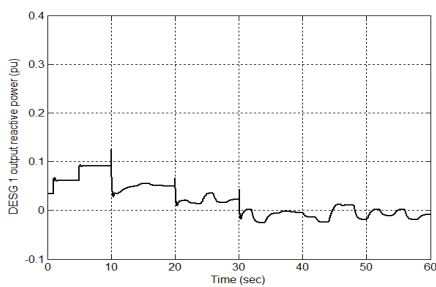
(d) DESG1 reactive power
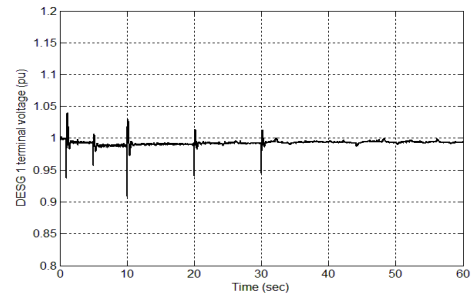
(e) DESG1 terminal voltage
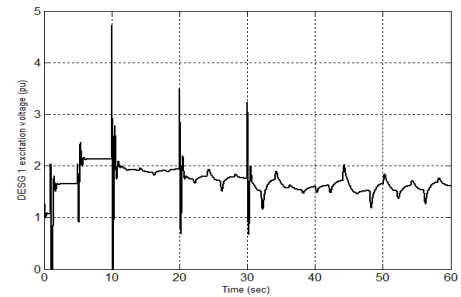
(f) DESG1 excitation voltage

Fig. 8 Variations of variables of diesel engine power generation system
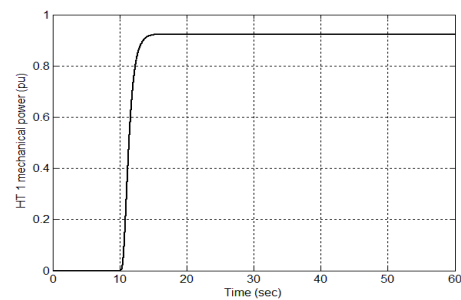
(a) SHT mechanical power
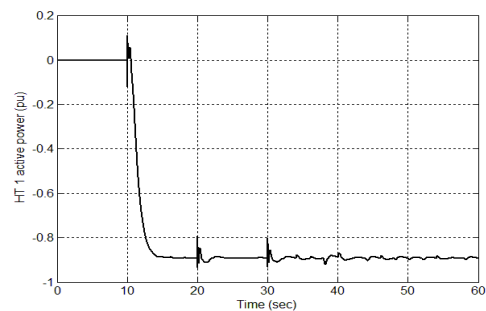
(b) HTIG active power
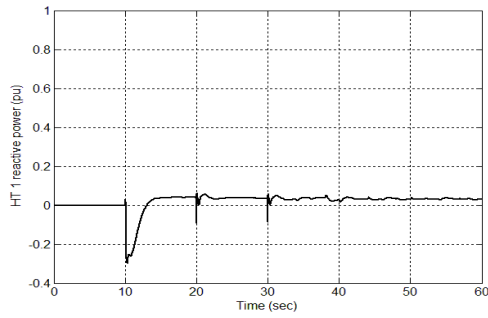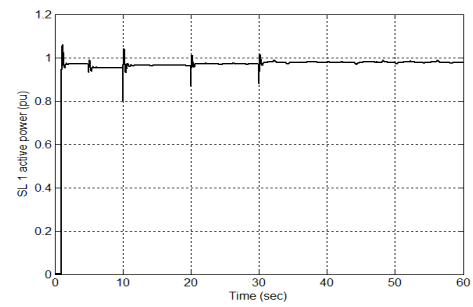
(c) HTIG reactive power
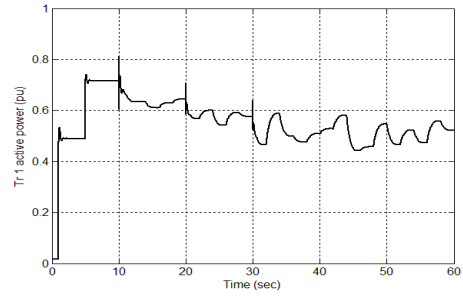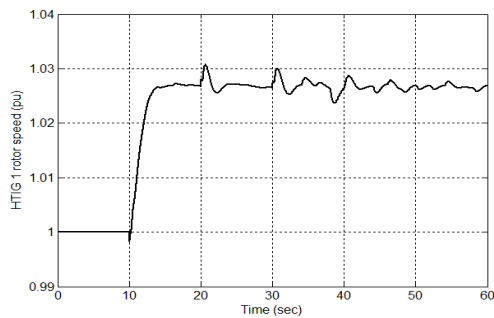

(a) SGTr1 active power
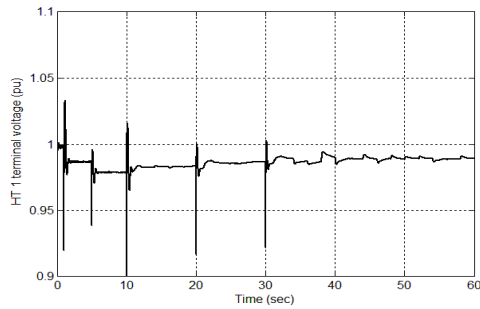
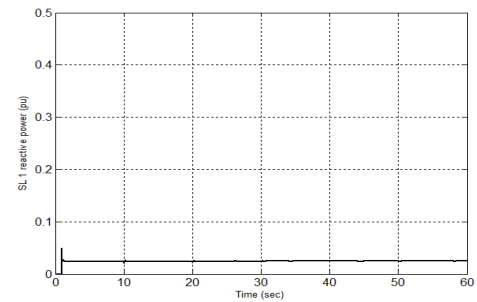

(d) HTIG terminal voltage
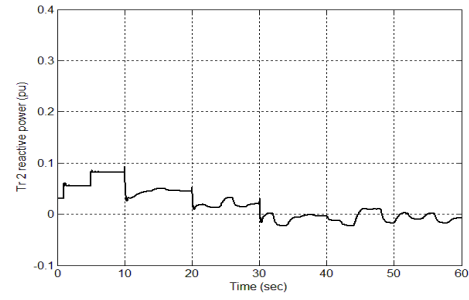
(b) SGTr1 reactive power
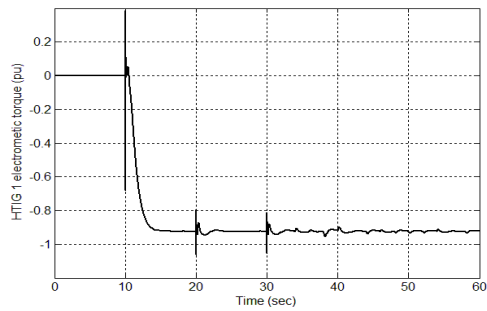
(e) HTIG electromagnetic torque

(c) SL1 active power
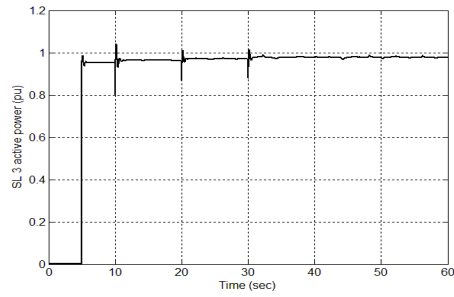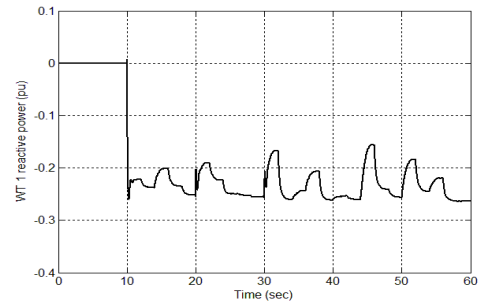

Fig. 9 (f) HTIG rotor speed

Fig. 9 Variations of variables of small hydraulic power generation system
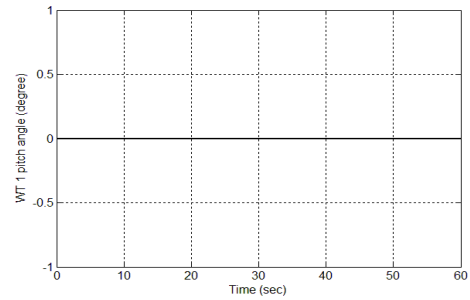

(d) SL1 reactive power

(e) Static load SL2 active power
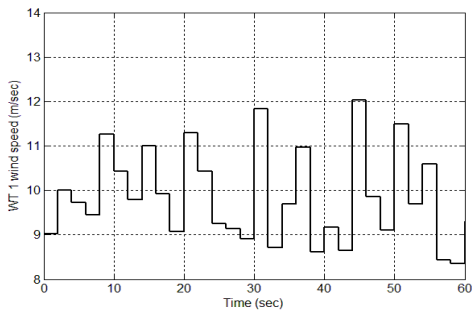
(c) WT1 reactive power
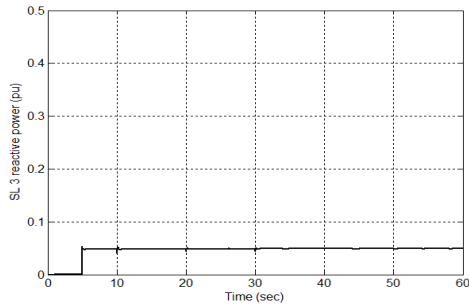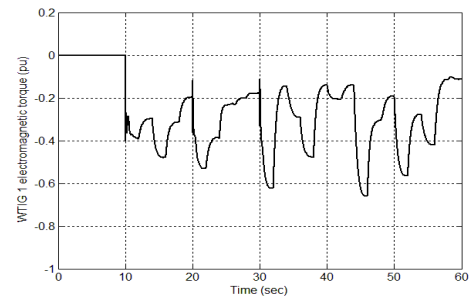
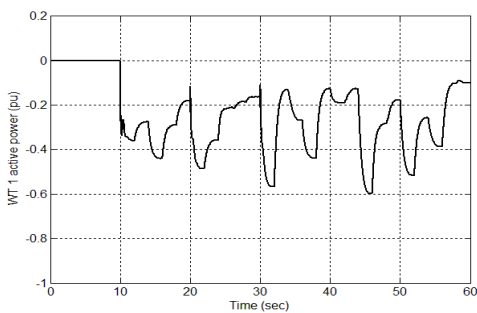(f) SL2 reactive power

(d) Wind turbine WT1 pitch angle

Fig. 10 Variations of variables of transformers and static loads

(a) WT1 wind speed

(e) WTIG1 electromagnetic torque
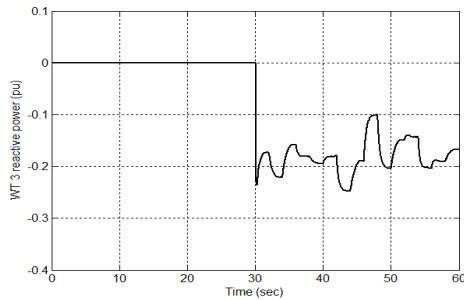
(b) WT1 active power
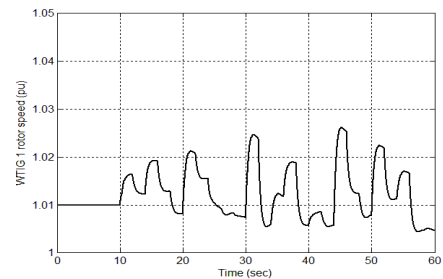
(f) WTIG1 rotor speed

Fig. 11 Variation of variables of the first wind turbine

(a) WT2 wind speed

(b) WT2 active power

(c) WT2 reactive power

(d) Wind turbine WT2 pitch angle

(e) WTIG2 electromagnetic torque

(f) WTIG2 rotor speed

Fig. 12 Variation of variables of the second wind turbine

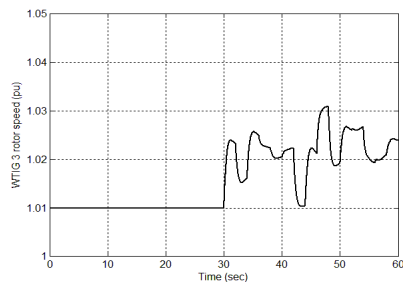(a) WT3 wind speed

(b) WT3 active power

(c) WT3 reactive power
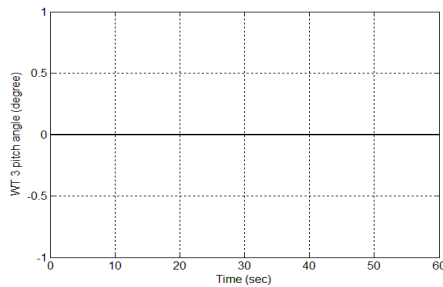
(d) Wind turbine WT3 pitch angle
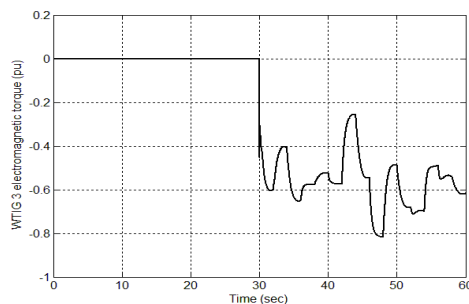
(e) WTIG3 electromagnetic torque

(f) WTIG3 rotor speed

Fig. 13 Variation of variables of the third wind turbine

IV. DISCUSSIONS

The purpose of this study was to realize the dynamic behavior of an island power system under random wind speed lower than nominal wind speeds of wind turbines. The results show the output power of diesel engine power generation systems was 0.8pu when static loads were connected and

decreased to around 0.55pu after the renewable energy power generation systems had supplied power to the system. The power shared by the renewable energy power systems reached 0.25pu accounting for a penetration of 45%. The pitch angle of wind turbines was not adjusted because the wind speeds were less than the nominls of wind turbines. The output power of wind turbine fluctuated with the variation of wind speed. In contrast, the output power of small hydraulic turbine was stable due to the constant water flow. Overall, the system can run stably in this operational mode, and the variations of system variables are reasonable. The research results are coincident with expectation.

V. CONCLUSIONS

The objective of this study was to investigate the dynamic behavior of an island power system under random wind speed. The results suggested the system can operate stably in this operational mode. This study can serve as an important reference for planning, operation, and further expansion ofisland power systems. Future studies will include other renewable energy systems such as photovoltaic system and variable-speed wind turbine for more understanding of their influence on the dynamic behavior of island power systems.

REFERENCES

[1] http://www.moeaboe.gov.tw/Policy/98EnergyMeeting/conclusion/concl usion_3.html.
[2] Taiwan Power Company, http://www.taipower.com.tw.
[3] Borbely, J. Kreider, *Distributed Generation: The Power Paradigm for the New Millennium*, CRC Press, 2001.
[4] T.K. Saha and D. Kastha, "Design Optimization and Dynamic Performance Analysis of a Stand-Alone Hybrid Wind-Diesel Electrical Power Generation System," *IEEE Transactions on Energy Conversion,* vol. 25, no. 4, pp. 1209-1217, Dec. 2010.
[5] K. Uhlen, B.A. Foss, and O.B. Gjosater, "Robust Control and Analysis of a Wind-Diesel Hybrid Power Plant," *IEEE Transactions on Energy Conversion*, Vol. 9, Dec. 1994, pp.701-708.
[6] P. Sharma and T. Bhatti, "Performance Investigation of Isolated Wind-Diesel Hybrid Power Systems with WECS having PMIG," *IEEE Transactions on Industrial Electronics*, Vol. PP, Issue 99, pp. 1-8, 2011
[7] S.S. Murthy, S. Mishra, G. Mallesham, and P.C. Sekhar, "Voltage and Frequency Control of Wind Diesel Hybrid System with Variable Speed Wind Turbine," *2010 Joint International Conference on Power Electronics, Drives and Energy Systems (PEDES)*, 2010, pp. 1-6.
[8] H. Sharma, S. Islam, C.V. Nayar, and T. Pryor, "Dynamic Response of a Remote Area Power System to Fluctuating Wind Speed," *IEEE Power Engineering Society Winter Meeting*, Vol. 1, Jan. 2000, pp.499-504.
[9] S.A. Papathanassiou and F. Santjer, "Power-Quality Measurements in an Autonomous Island Grid with High Wind Penetration," *IEEE Transactions on Power Delivery,* vol. 21, no. 1, pp. 218-224, Jan. 2006
[10] E. Muljadi and H.E. McKenna, "Power Quality Issues in a Hybrid Power System," *IEEE Transactions on Industry Applications,* Vol. 38, No.3, May/June 2002, pp.803-809.
[11] R.C Bansal, T.S Bhatti, and D.P. Kothari, "Automatic Reactive Power Control of Wind-Diesel-Micro-Hybrid Autonomous Hybrid Power Systems Using ANN Tuned Static Var Compensator," *Large Engineering Systems Conference on Power Engineering*, May 2003, pp.182-188.
[12] R. Sebastian, M. Castro, E. Sancristobal, F. Yeves, J. Peire, and J. Quesada, "Approaching hybrid wind-diesel systems and Controller Area Network," *IECON 02*, Vol. 3, Nov. 2002, pp.2300-2305.
[13] J. Delesalle and I. Kauffmann, "Réponse Des Moteurs Diesel Suralimentés Aux Variations Rapides De Puissance Appelée Simulation Mathématique Et Applications," *CIMAC*, A, 1977, Pap. A9.
[14] J.R. Smith, A.F. Stronach, and T. Tsao, "Digital simulation of marine electro-mechanical drive systems," *IEEE Transactions on Industry Applications*, IA-18, 1982, pp.393-399.

[15] S. Heier, *Grid Integration of Wind Energy Conversion Systems*, *2nd Ed*, John Wiley & Sons Ltd., June 2006.

[16] P. M. Anderson and A. Bose, "Stability Simulation of Wind Turbine Systems," *IEEE Transactions on Power Apparatus and Systems*, Vol. 102, No. 12, pp.3791-3795, Dec. 1983.

[17] P.C. Krause, *Analysis of Electric Machinery and Drive System, 2nd Ed,* McGRAW-Hill Book Co., USA, Dec 2001.

[18] C.-M. Ong, *Dynamic Simulation of Electric Machinery using MATLAB/Simulink*, McGRAW-Hill Book Co., USA, 1998.

[19] IEEE Committee Report, *IEEE Guide for Identification, Testing and Evaluation of the Dynamic Performance of Excitation Control Systems*, ANSI/IEEE Std 421A-1987, June 1978.

[20] IEEE Committee Report, "Excitation System Models for Power System Stability Studies," *IEEE Transactions on Power Apparatus and Systems,* PAS-100, 1981, pp.494-509.

[21] *Using Simulink*, the Mathworks Inc., 2009.

[22] *SimPowerSystems User's Guide,* Hydro-Quebec TransEnergie International, 2009.

Meng-Jen Chen was born in Taiwan, R.O.C. He received the Diploma in Electrical Engineering from the National Kaohsiung Institute of Technology, Taiwan and Ph.D. degree in Electrical Engineering from the University of Strathclyde, Glasgow, UK, in 1984 and 1992, respectively. Since 1992, he has been an Associate Professor in the Department of Electrical Engineering, National Kaohsiung University of Applied Sciences, Taiwan. His research interests include wind energy conversion systems, photovoltaic power systems, distributed power systems, and smart microgrid.

Yu-Chi Wu (M'93–SM'99) received the Electrical Engineering Diploma in 1984 from the National Kaohsiung Institute of Technology, Taiwan, the M.S. and Ph. D. degrees both in 1993 from the Georgia Institute of Technology (Georgia Tech), U.S.A. He has been involved in activities in both academic and industrial areas since 1986. His industrial work experience with Pacific Gas and Electric Company, EDS/Energy Management Associates, and EDS/China Management Systems includes development and study of EMS applications and power system planning. Now he is a professor at the Department of Electrical Engineering, National United University, Taiwan.